Raghuram et al., http://www.jcb.org/cgi/content/full/jcb.201305159/DC1

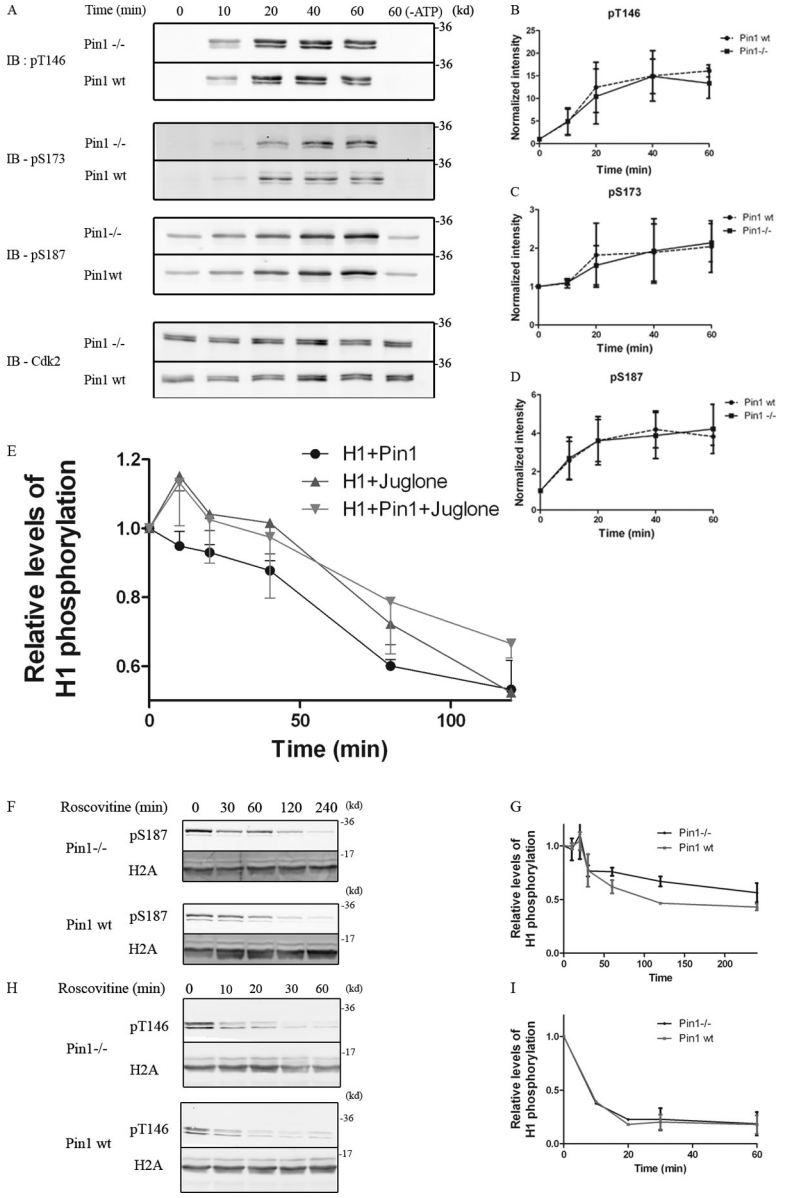

Figure S1. **Kinetics of Cdk2 extracted from Pin1wt and Pin1$^{-/-}$ cells.** (A) Cdk2 was immunoprecipitated from either Pin1$^{-/-}$ cells or Pin1wt cells and diluted in H1 kinase buffer along with purified H1 ± ATP. The phosphorylation reaction was stopped at regular time intervals with the addition of SDS loading buffer. The extracts were then run on 18% acrylamide gels and probed for changes in pT146, pS173, and pS187 levels. The changes in the intensity are plotted in B–D, with the intensity measured at time zero, set to 1. (E) In vitro inhibitor of Pin1, Juglone, abrogates the enhanced rate of H1 dephosphorylation in the presence of Pin1. Juglone was used at a concentration approaching 10 molar equivalents to every mole of Pin1.

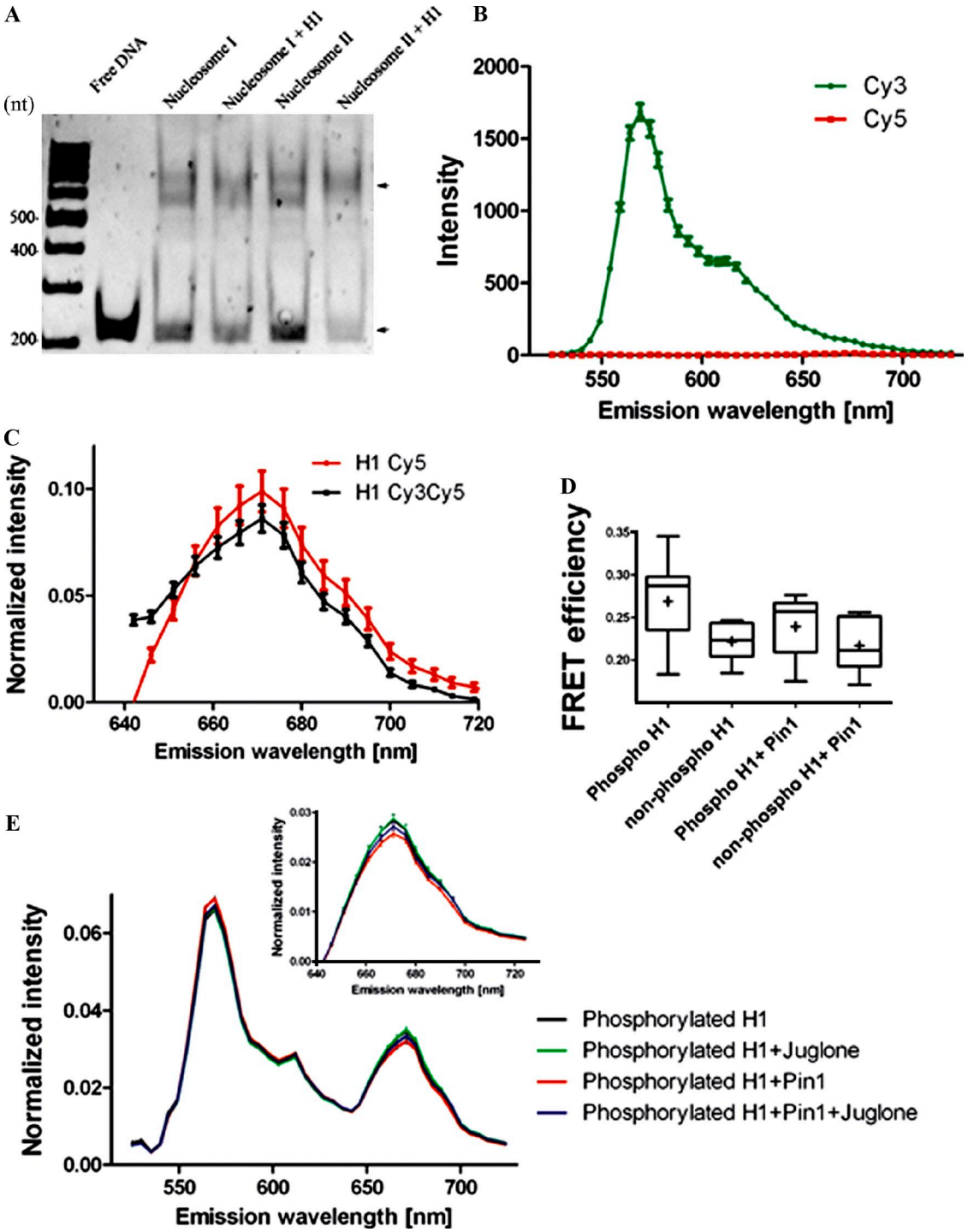

Figure S2. **FRET controls and FRET efficiency.** (A) Nucleosome reconstitution was performed as described in Materials and methods. Free DNA and two different batches of reconstituted nucleosomes were run on 5% native gels with 0.5% TBE running buffer. H1Cy3Cy5 were added in a 1:1 molar stoichiometry in samples run on lanes 4 and 5. Addition of nucleosomes causes a characteristic shift in the migration of DNA around the 600-bp mark. (B) H1Cy3 and H1 Cy5 emission spectra when excited with a 514-nm laser. Note that there is very little emission of Cy5 at the 671-nm range (peak for Cy5), whereas there is a slight "shoulder" still present for Cy3 emission spectra at this wavelength. (C) H1Cy5 and H1Cy3Cy5 emission spectra when excited with a 633-nm laser. Similar emission spectra suggest that the addition of a Cy3 tag does not interfere with Cy5 emission. (D) Changes in FRET efficiencies upon phosphorylation of H1 and addition of Pin1 in H1Cy3Cy5 constructs. Formula for the measurements can be found in Materials and methods and references within. Plus sign indicates the mean, and median is represented by the horizontal line in between the boxes. (E) Changes in CTD FRET were significantly reduced when in vitro inhibitor of Pin1, Juglone, was added to the mixture of H1Cy3Cy5 and Pin1, in the presence of nucleosomes. Note that in the presence of Juglone and Pin1, the spectrum tends to approach the emission spectrum characteristic of just-phosphorylated H1.

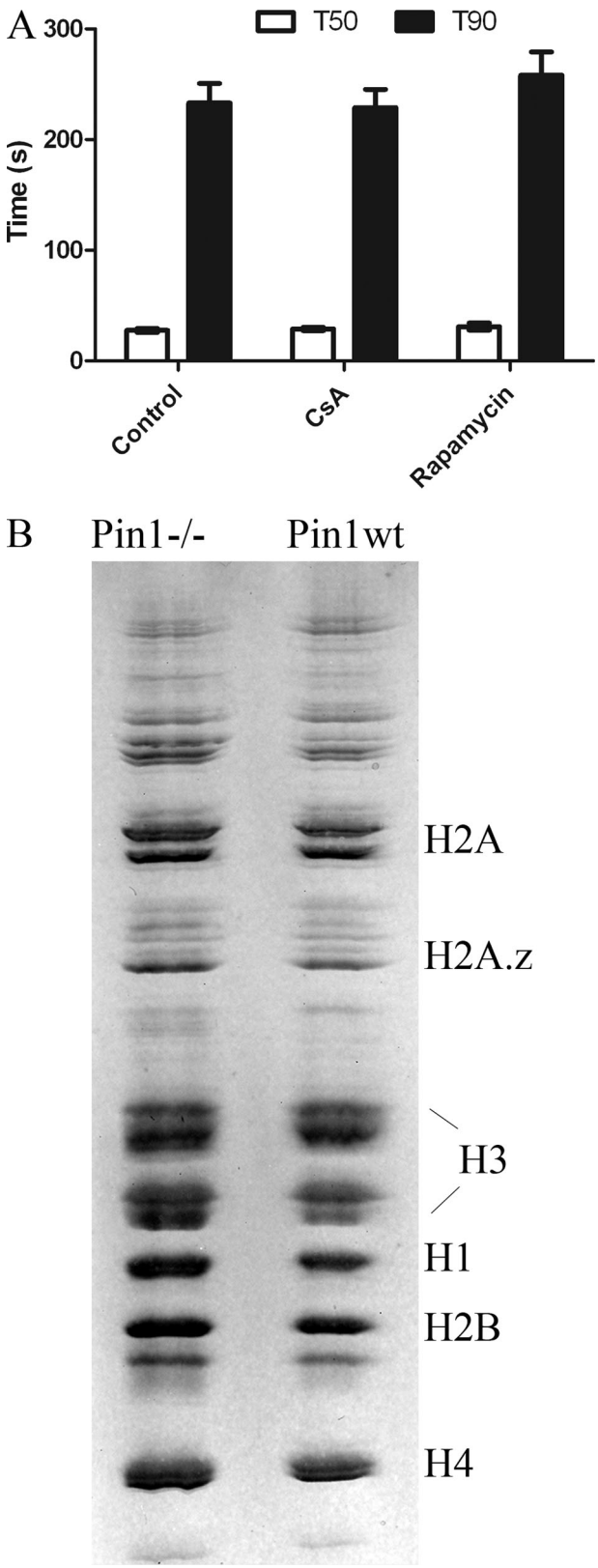

Figure S3. **Phosphorylation-independent proline isomerization does not alter H1 binding.** (A) Effect of cyclosporine and rapamycin on H1 dynamics. GFP H1.1 was transfected in 10T1/2 mouse embryonic cells and was treated with either 1 h of cyclosporine A or rapamycin, after which H1 dynamics was measured with FRAP. T_{50} and t_{90} values were quantified; however, there were no statistically significant changes in the dynamics of H1 after such treatment. (B) Core histone and H1 composition in Pin1wt vs. Pin1$^{-/-}$ cells. Histones were extracted from Pin1$^{-/-}$ cells and Pin1wt cells using 0.4 N H_2SO_4 and run on an acetic acid–Urea–Triton X-100 (AUT; 15% separating). AUT gels separate the proteins based on charge and mass. Core histone composition and other post-translational modifications, such as acetylation of H4 (which usually appears as ladders), were found to be very similar.

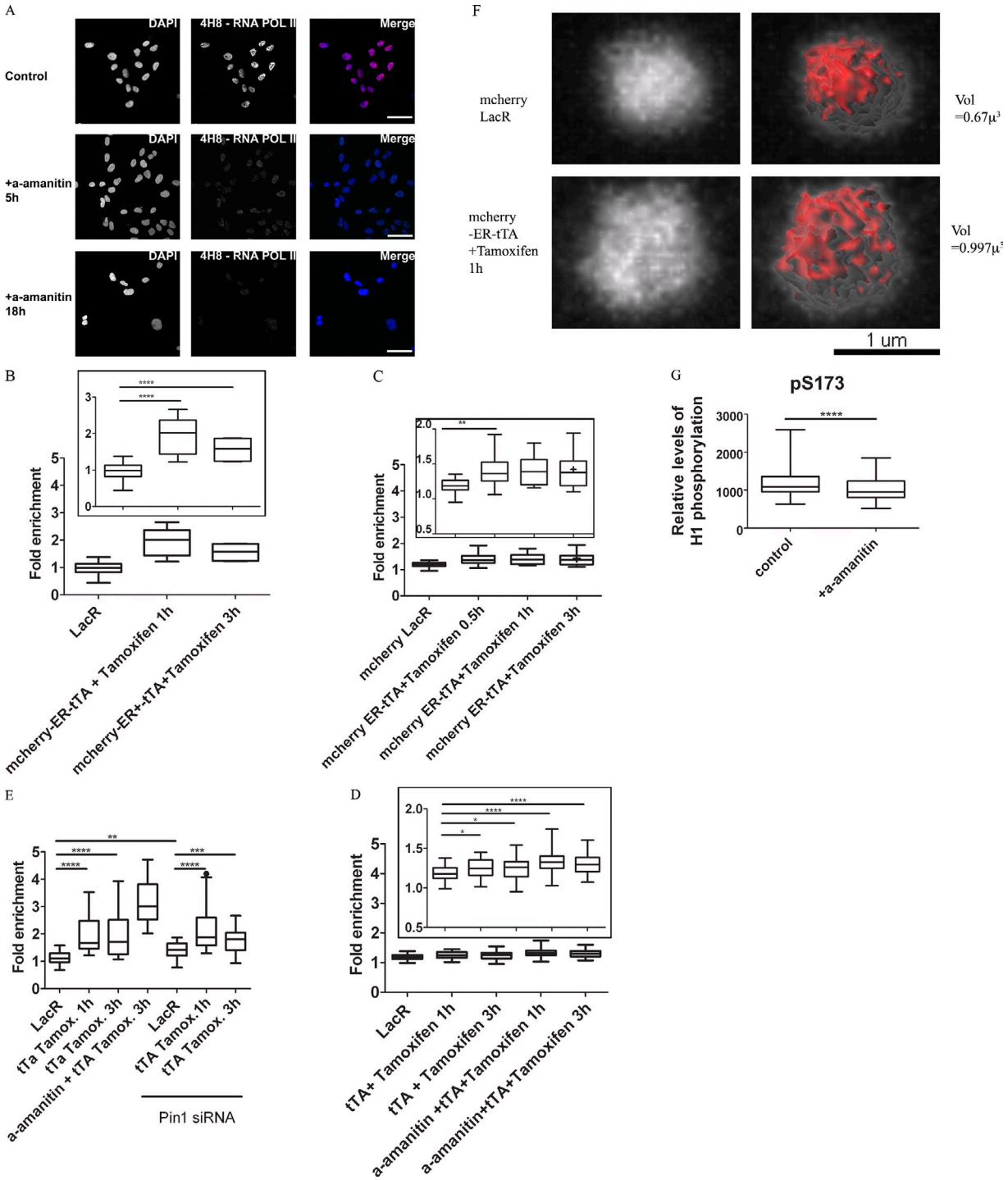

Figure S4. **Accumulation of RNA polymerase II at sites of transcription and the effect of α-amanitin on its levels.** (A) U2Os 263 cells were treated with α-amanitin for either 5 or 18 h in order to deplete the pool of RNA polymerase II. At the 5-h time point, some RNA polymerase II foci were still observed; however, at the 18-h time point these were significantly reduced. Bar, 50 µm. (B) Quantification of RNA polymerase II after addition of tamoxifen at lac arrays (n = 36). (C) Quantification of YFP-MS2 at sites of transcription after addition of tamoxifen (n = 20, from three independent experiments, with the horizontal line in the floating bars [min/max] representing the median). This is used as readout for transcriptional elongation. pS173 H1.2 levels (D) and Pin1 levels (E) were measured by using the mCherry-LacR or mCherry-ER-tTA as a mask to define regions of interest. The intensity obtained from this channel was measured against the average intensity of the entire nucleus to obtain fold enrichment. Each dataset is an average value reported from more than 30 cells compiled from two or more independent experiments. These experiments clearly show the increase in Pin1 levels and pS173 levels at sites of transcription, with this increase being independent of RNA polymerase II. (F) U2Os 263 cells were transfected with either mCherry LacR or mCherry-ER-tTA, after which transcription as induced with the help of tamoxifen. These cells (living) were then placed under a confocal microscope and subject to z-stacks (50 slices in 9 s). The stacks were then analyzed on Imaris surface-rendering software and the volume occupied by the arrays was measured. Examples illustrated here show the "puffing" of the arrays upon transcriptional induction. The average volume (more than 60 cells) increases from 0.67 μ^3 to 0.997 μ^3 upon activation of transcription. (G) Relative levels of pS173 levels after depletion of RNA polymerase II levels by treatment with α-amanitin (18 h). Notation for significance: *** if P value is < 0.001; ** if P is between 0.001 and 0.01; * if P is between 0.01 and 0.05.

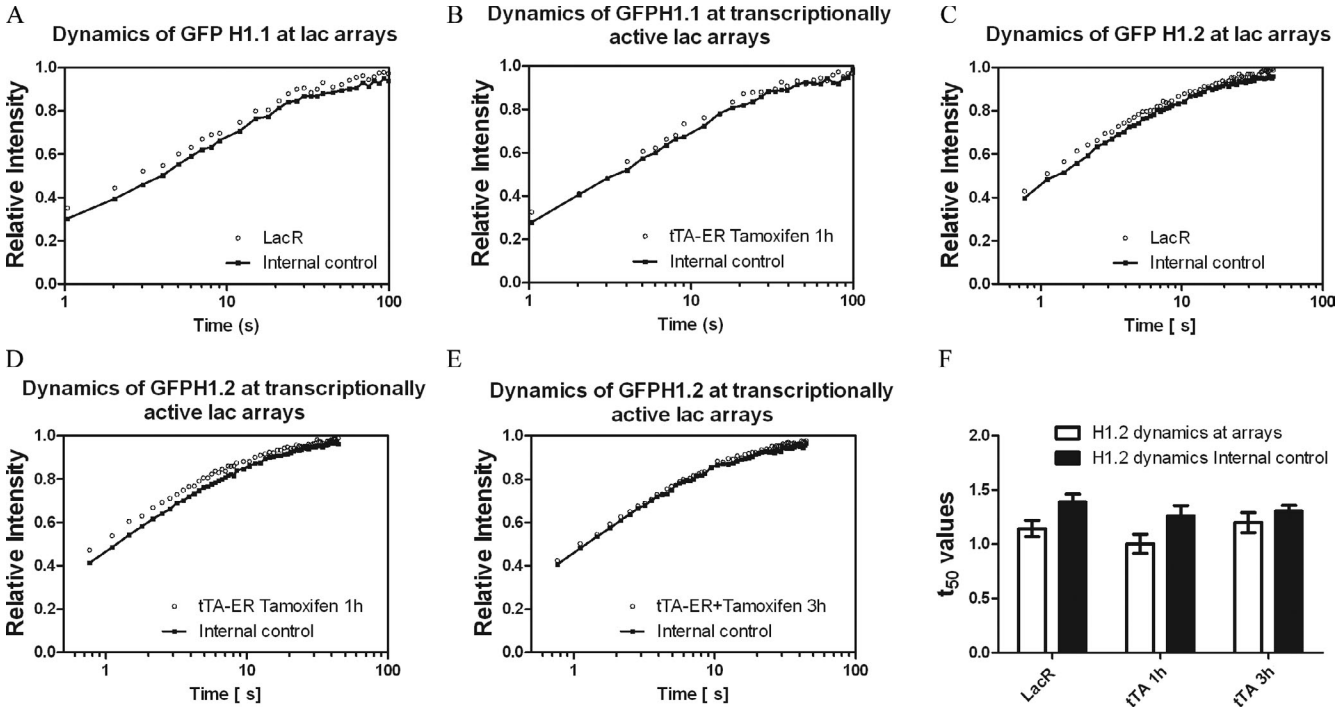

Figure S5. **Dynamics of H1.1 and H1.2 at sites of transcription.** U2OS 263 cells were cotransfected with either GFP H1.1 or GFP H1.2 and mCherry LacR or mCherry-ER-tTA. The dynamics of GFPH1.1 was measured at the lac arrays at transcriptionally inactive sites (A) and when the same was activated with transcription (B) with tamoxifen (1 h). Similarly, the dynamics of another euchromatin-enriched H1 variant H1.2 was measured at transcriptionally inactive sites (C), and when transcriptionally activated with tamoxifen for 1 h (D) and 3 h (E). The t_{50} values from the FRAP curves are shown in F. Each FRAP curve represents an average of ~30 unique sites of transcription from three independent experiments.